Balloon Tuning Technique for SRF cavities

Fermilab Summer Student Program, 2016

Alessandro Tesi

University of Pisa

Supervisor:

Donato Passarelli

Co-Supervisor:

Mohamed Hassan

October 10, 2016

Abstract

A novel tuning solution for dressed superconducting radio-frequency cavities is presented. The study has focused on the tuning procedure validation process, by means of numerical simulations and experimental tests.

Contents

List of Figures

1 Introduction

The subject of the present study is the validation of a novel tuning technique for multi-cell superconducting radio-frequency cavities, i.e. the Balloon Tuning Technique. In the following sections, a brief explanation of the problems connected to the cavity tuning is presented, as well as the principal features and advantages of our innovative solution.

1.1 Tuning of SRF cavities

Superconducting radio-frequency (SRF) cavities have a huge impact in the particle accelerator science because of their ultra-low loss that extremely enhances their efficiency in accelerating particle beams.
The importance of keeping an SRF cavity at the exact *frequency of resonance* is crucial to the operation of an entire particle accelerator. For this reason, many solutions are being developed to passively and actively compensate frequency detuning in SRF cavities. The control of the resonant frequency of a cavity in operation is usually achieved by slightly deforming the structure in the linear-elastic regime of niobium, preventing plastic deformations. On the other hand, an inelastic tuning is performed when the cavity is not under operation.
At the same time, having equal electromagnetic field amplitude in the different cells of a multi-cell cavity is crucial to achieve the desired values of accelerating gradient. This feature is typically expressed by the parameter *field flatness*, which is defined as the ratio between the lowest and the highest axial electric field amplitude in the different cells of a cavity. A flat field profile is usually achieved when the cells are properly tuned relative to each other and the cavity frequency is equal to the designed value. The main problem is that the currently available manufacturing process cannot guarantee a sufficient grade of precision for both resonant frequency and field flatness; moreover, a cavity may experience a field flatness deterioration during some preliminary treatments and preparation steps. In practice, the discrepancy between the ideal and real RF field flatness is mitigated by permanently deforming the niobium structure in certain areas.
The above mentioned inelastic tuning approach is quite mature for bare cavities [1], but similar adjustment techniques are inefficient and expensive for dressed ones, where the niobium structure is not easily accessible (Fig. 1). When a dressed cavity shows field flatness

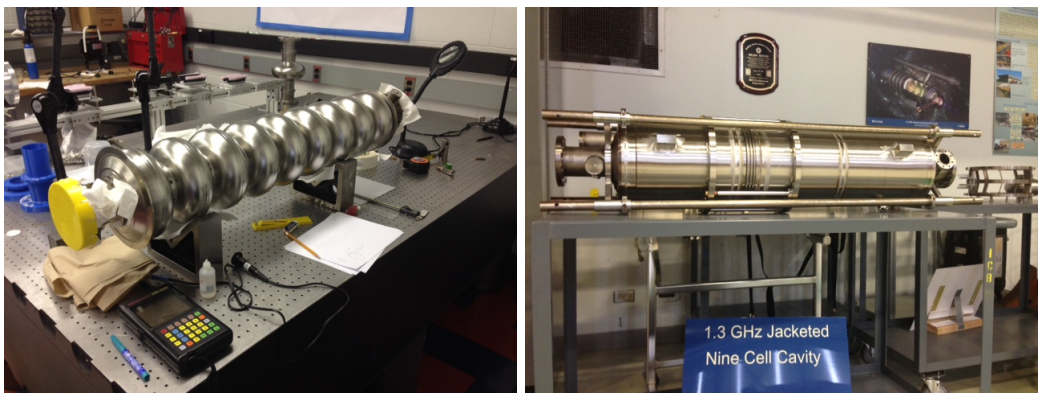

(a) (b)

Figure 1: Bare (a) and dressed (b) cavities.

issues, indeed, the current solution consists of removing the outermost vessel, fixing the frequency and the field flatness by means of the tuning machine and then welding a new helium tank around the cavity. The whole procedure is delicate, full of risk and very expensive ($\sim$ 200k USD). For instance, during the LCLS-II experiment at Fermilab, a dressed cavity accidentally suffered a plastic deformation during the insertion in the cryomodule. As a consequence, the cavity experienced a field flatness deterioration with the result of

not being usable anymore. Considering the cost of a dressed cavity ($\sim$ 250k USD) and the complexity of the adjustment techniques, a huge economic damage arose from that mistake. The lesson to be learnt from the mentioned accident is that innovative tuning techniques should be investigated to have an easy way for a dressed cavity retuning and field correction.

1.2 BTT general features

The Balloon Tuning Technique (BTT) may represent a tuning solution for dressed multi-cell cavities, capable of controlling the deformation of each single cell. The proposed method relies on pressurizing balloons inside the non operating cavity to lower than maximum allowable working pressure and mechanically applying a force on the end flange, using existing mechanical tuner devices. The goal of each tuning step is to produce a permanent change in the iris-to-iris distance of a targeted cell. When compressing a targeted cell, a decrease in the iris-to-iris distance produces a decrease in both the cavity resonant frequency and the cell field amplitude. When expanding a cell instead, an increase in both the cavity resonant frequency and the cell field amplitude is produced. As it usually happens also in the classic tuning techniques, the desired physical properties of the whole resonating structure are achieved after several iterations on each cell. As a result, a significant improvement of the field flatness (above 90%) is expected, while the resonant frequency should be maintained within the acceptable range of the specific cavity.
Unlike the majority of the currently used tuning techniques, the BTT performs a field flatness adjustment and a frequency retuning acting from the inside, as previously stated. This is a key point that would allow the procedure to be potentially effective not only on bare cavities, but also on dressed ones, whose field correction would not require a complex and expensive undressing procedure anymore.
A remarkable economic advantage may arise from the successful validation of the Balloon Tuning Technique, because the cost of this tuning solution including hardware, software and operation ($\sim$ 40k USD) will be negligible compared to the cost of only one dressed multi-cell adjustment. In this regard, the impact of a production failure in a large-scale leading project such as PIP-II and LCLS-II would be minimized from cost and scheduling standpoints.

1.3 Operating procedure

In the following section, a detailed description of the BTT principles of operation is reported. A bare 9-cell 1.3 GHz cavity model has been used for the method description and the further analysis.
First, a preliminary measurement of the resonant frequency and field flatness should be performed in order to qualify the cavity and eventually detect the first targeted cell to operate on. As a second step, the targeted cell compression or expansion takes place according to the measurement results. As the real tuning operation is completed, a new qualification of the modified cavity parameters is needed to verify the achieved results and choose the following targeted cell. The cycle is then repeated until the desired electromagnetic properties are finally achieved and the cavity is ready for operation.

1.3.1 Cell compression

Suppose one targeted cell, e.g. cell 4, needs to be compressed, in order to produce a decrease in both the cavity resonant frequency and the cell field amplitude.
A set of deflated balloons are folded and placed in all the other cells of our non operating cavity, as shown in Fig. 2. The balloons then get pressurized, so as to produce a pressure on the inner wall of the non-targeted cells. At this point, a compression force is applied by a mechanical tuner device to the first end flange, while the other flange remains fixed (Fig. 3). The targeted cell experiences the entire effect of the compression force, whereas in all the other cells the force effect is mitigated by the balloon-produced pressure. As a result, a higher stress state is expected in the targeted cell, whereas a lower stress state should be observed in all the other ones. This differential stress is the key of the whole deformation-based tuning mechanism: by choosing a suitable combination of applied force

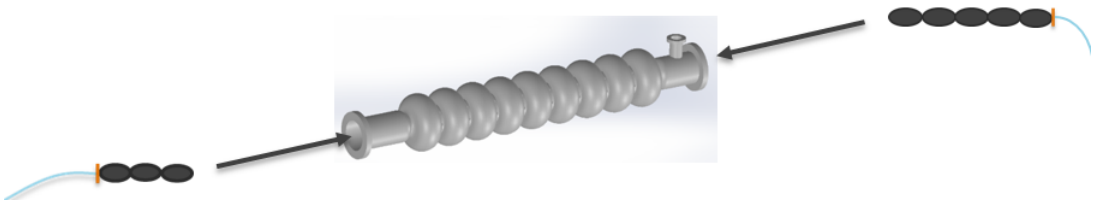

Figure 2: Deflated balloons are placed in the non-targeted cells for the compression of cell 4.

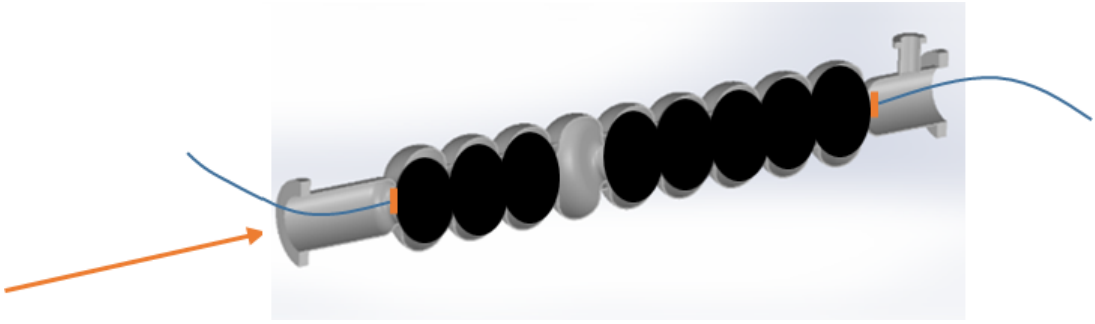

Figure 3: Cell 4 compression is executed.

F and balloon pressure P, indeed, the targeted cell stress value may overstep the niobium yield point, while the stress value observed in the non-targeted cells may remain under that point. Consequently, a plastic deformation in the targeted cell and an elastic one in all the other cells may be achieved.
As a final result, after the removal of the external load and the balloon set, a complete elastic recovery occurs in the non-targeted cell, while a permanent decrease in the targeted cell iris-to-iris distance has been produced.

1.3.2 Cell expansion

Suppose now one cell iris-to-iris distance must be expanded, so as to increase the cavity resonant frequency and the cell field amplitude.
One deflated balloon is folded and inserted into that targeted cell (Fig. 4). Then, the

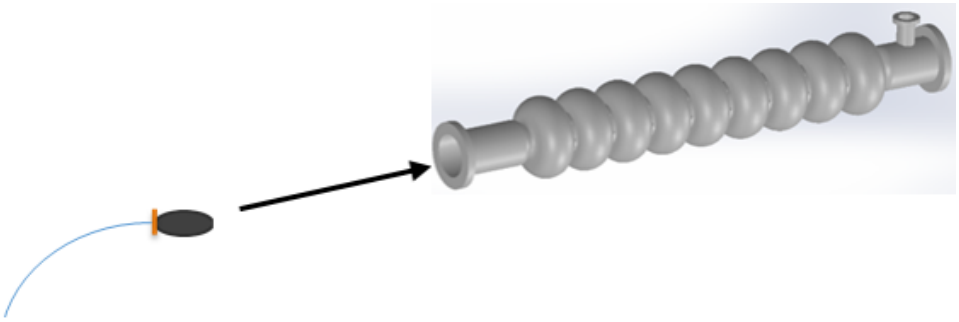

Figure 4: A deflated balloon is inserted into the cell that must be expanded.

balloon is pressurized so as to apply a pressure to the inner wall of the cell. A traction force is applied by the tuner to the first end flange, while the other one remains fixed again (Fig. 5). The combined effect of the traction force and the balloon pressure produces a higher stress state in the targeted cell, which may get plastically deformed under the assumption of working in proximity of the niobium yield stress. Since all the other cells experience just the traction force, they remain in the linear elastic region instead. Again, after the removal

of the external load and the balloon, the produced differential stress will have brought to a complete shape recovery in the non-targeted cells and to a permanent increase in the targeted cell iris-to-iris distance.

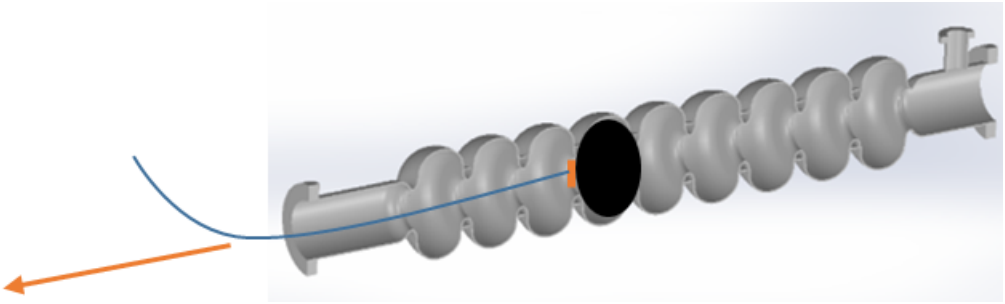

Figure 5: The targeted cell expansion is executed.

2 Numerical simulations

In order to demonstrate the validity of the proposed approach, a Finite Element Analysis (FEA) has been performed by means of COMSOL Multiphysics Software.
Several mechanical simulations were needed to verify the existence of that differential stress which is required to bring the targeted cell in the niobium plastic deformation regime and to allow all the other cells to remain in the linear-elastic one. Moreover, a study has been performed to detect the appropriate ranges of external force and balloon pressure capable of producing that useful condition.
A Multiphysics analysis was then required to simulate how the mechanical deformation of one cell affects the cavity frequency shifting during the loading process.
Similar results were expected for middle cells (2-8), while slightly different ones were expected for end cells (1, 9) due to edge effect and asymmetry. In the following sections, FEA results are reported for a middle cell study, e.g. cell 4. The end cell behavior has been investigated, but the corresponding results will be mentioned just when differences are not negligible.

2.1 Mechanical simulations

Mechanical simulations have been dedicated to each single cell separately, for both compression and expansion cases. The nominal geometry of a bare ILC 9-cell 1.3 GHz cavity has been used, and just one quarter of the whole structure was modeled because of the symmetry, in order to limit computational time and complexity. Although the BTT application presents its major advantages in the tuning of dressed cavities, a bare one was used in the numerical simulations and the following experimental tests, because of cost factors.
A linear and stationary simulation setup was considered sufficient at the early stage of the validation process from a mechanical standpoint. Further studies shall include the non-linear behavior that niobium exhibits over its yield stress, i.e. 70 MPa; moreover, a time dependent simulation would be crucial to have a deeper understanding of the loading dynamics. However, meaningful data could be extracted at this point from the analysis of niobium stress strain curve [2], such as the amount of permanent deformation produced on a targeted cell by the tuning procedure.
In all our mechanical simulations, a cross parametric sweep has been performed over those parameters defining the procedure working point, such as the tuner force and the balloon pressure:

- F between 2 and 8 kN
- P equal to 1.5, 2 and 2.5 bar.

Once we have studied the results produced by all the possible combinations of F and P, it will be easy to choose a proper operating couple (F, P) in order to have the method being effective.

2.1.1 Cell compression

A pressure P has been applied to the inner wall of the non-targeted cells, with the aim of reproducing the balloon pressurization effect. At the same time, a compression force F has been applied to one end flange, while the other one has been fixed by a zero displacement constraint along the axial direction.

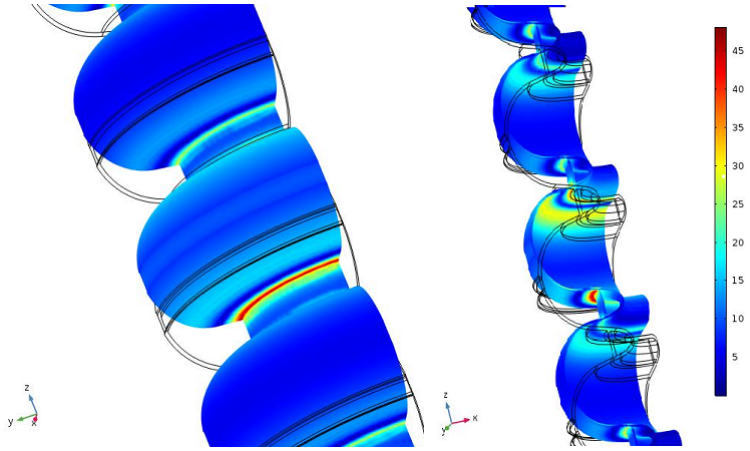

(a) (b)

Figure 6: External (a) and internal (b) view of the surface von Mises stress distribution during a mid cell compression.

The simulation result proves that a higher stress state appears in the targeted cell walls, as expected. In Fig. 6, the surface plot of the von Mises stress is reported for the cell 4 compression loading process, with a balloon pressure of 2.5 bar and a compression force of 4 kN. As it appears from both the internal and the external view, the stress is more pronounced in proximity of each cell iris, but a larger stress value is found precisely on the iris of the targeted cell; this peculiar stress distribution is exactly what we need in order to perform the frequency retuning as well as the field flatness adjustment. A 2D plot of the von Mises stress along the cavity profile is reported in Fig. 7, with the aim of representing the mentioned stress distribution in a more analytic way. The graph exhibits some stress spikes localized in each cell iris and confirms the existence of the differential stress produced by the balloon pressurization. For this reason, this graph may be considered as a preliminary evidence of the method validity from a mechanical standpoint.
An equivalent conclusion has been deduced from the simulations made on the end cells, as expected.

2.1.2 Cell expansion

At this time, pressure P has been applied to the inner wall of the targeted cell only, so as to reproduce the balloon pressurization effect. A traction force has been put on one terminal flange, while the other one was imposed a fixed constraint.
A 2D plot of the von Mises stress along the cavity profile is presented for the cell 4 expansion case as well, as shown in Fig. 8. The difference between the iris stress spike in the targeted and non-targeted cells is again proven to exist; therefore a first confirmation of the method validity can be derived for the expansion case.
Comparing the stress values we have obtained from all the mechanical simulations, we can state that a lower tuning force is required to produce an equal stress distribution in the

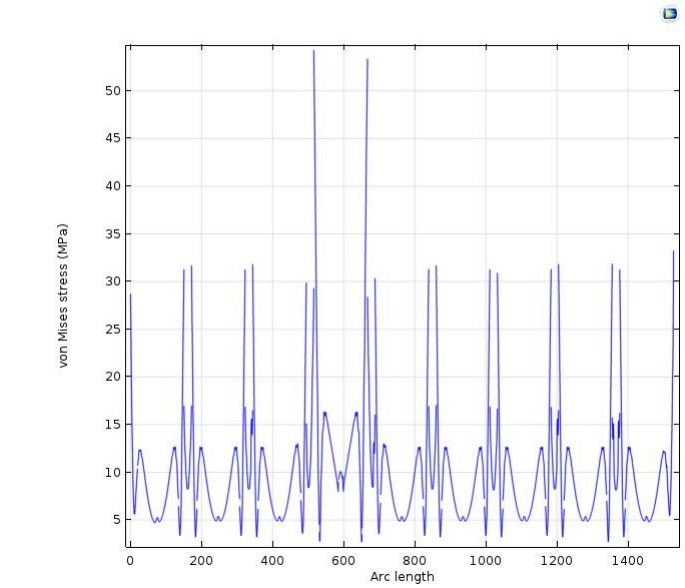

(a)

(b)

Figure 7: Plot (a) of the von Mises stress along the cavity external profile (b), produced by a cell 4 compression.

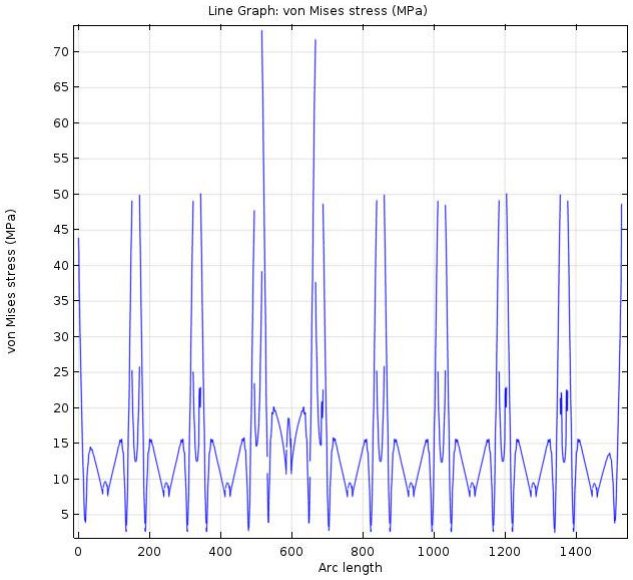

Figure 8: Plot (a) of the von Mises stress along the cavity external profile (b), produced by a cell 4 expansion; P = 2.5 bar, F = 4 kN.

expansion case, as reported in Sec. 2.1.5. This is due to the fact that the balloon pressure provides a positive contribution to the force effect during the expansion case, and not a negative one as it happens in the compression case instead.

2.1.3 Procedure figure of merit

As previously stated, our declared goal is to to achieve a plastic deformation in the targeted cell and an elastic one in all the others. Therefore, under the hypothesis of working around the niobium yield stress, it is of primary importance to have an as high as possible difference between the above mentioned iris-located stress spikes. This is the reason that brought us to define J, a procedure figure of merit. J is defined as the ratio between the stress spike observed in the targeted cell and the one observed in all the other cells. While working in an appropriate stress region, having a high J value means that the deformation procedure is clean, because the plastic deformation of the non-targeted cells is probably avoided while a permanent deformation of the target one is achieved.
In Fig. 9, a plot of J factor as a function of the loading force for different P values is presented (a), with reference to a mid cell compression process. A stress peak plot as a function of the applied force is included (b), in order to show which J value may be achieved when trying to obtain a precise stress on the targeted cell iris.

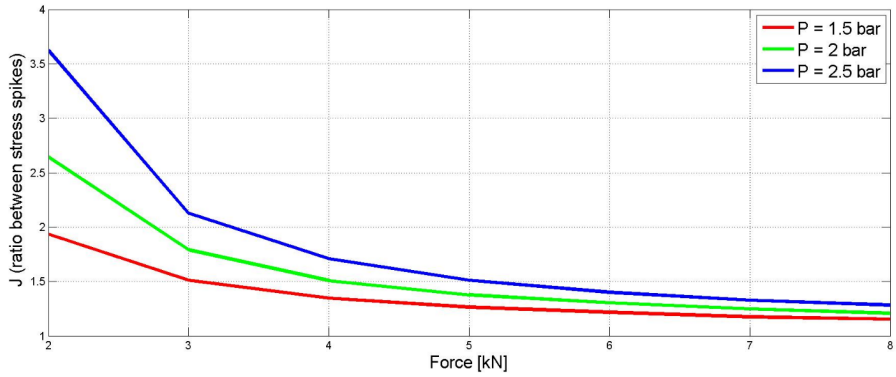

(a)

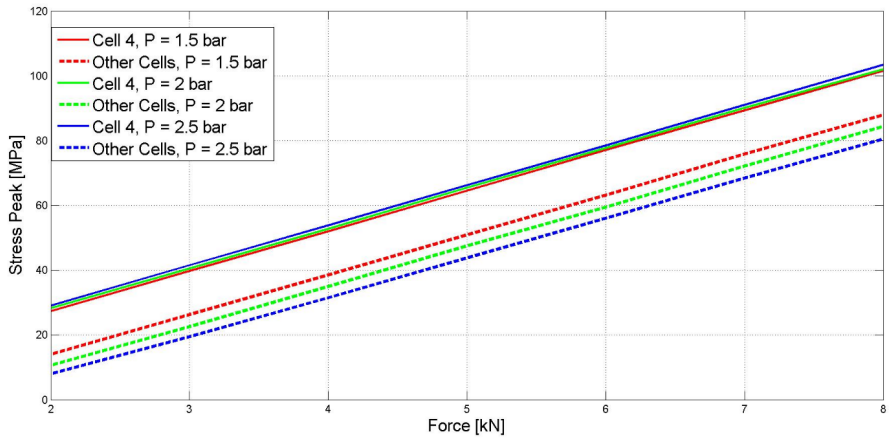

(b)

Figure 9: Plot of figure of merit (a) and stress peak (b) as a function of the applied force in cell 4 compression process.

A quick graph analysis suggests that the procedure figure of merit is maximized for high values of P and decreases with increasing values of F. This is due to the fact that the balloon pressure is the only responsible of the differential stress, considered that the external force acts on the whole structure and involves all the cavity cells. Moreover, the differential stress effect produced by the balloon pressure becomes more and more negligible as the force increases.
As a conclusion, enhancing the operating balloon pressure definitely facilitate a clean defor-

mation procedure. Nevertheless, a limitation to the pressure increase is obviously imposed by the resistance of the balloon material, as reported in Sec. 3.1.
The same study has been carried out for the expansion case, which exhibits a higher stress peak curve, combined to a lower value of J factor.
No significant differences have been found for an equivalent end cell investigation.

2.1.4 Cell stiffness estimation

An estimation of the cell stiffness has been performed in the mechanical analysis. Index K is defined as the ratio between the tuning force and the absolute cell length variation along the cavity symmetry axis. The estimated stiffness is equal to

- 33.33 kN/mm for a mid cell
- 37.24 kN/mm for an end cell.

These data could be useful for a theoretical estimation of the frequency shift produced by the tuning machine when further investigations will be performed.

2.1.5 Working point selection

Producing a permanent deformation on a targeted cell and preventing all the others from overstepping the linear-elastic limit is quite a delicate matter. Since the niobium yield stress is approximately 70 MPa, the goal of the loading process is to achieve:

- a peak stress value in the targeted cell iris > 70 MPa
- a peak stress value in all the other cell iris < 65 MPa.

When the balloon set is pressurized up to a certain pressure, a precise range of force is to be applied in order to obtain a reasonable tuning result. In Fig. 10, the search of a working point for cell 4 compression (a) and expansion (b) process is represented, under the hypothesis of a 1.5 bar balloon pressurization. In both graphs, a red line represents the iris-located stress peak of the targeted cell as a function of the external force, whereas the blue line has the same meaning but refers to the non targeted cells. Furthermore, the red arrow indicates the minimum force needed to produce the targeted cell plastic deformation, while the blue one indicates the maximum force we can apply to avoid the plastic deformation of all the other cells. In conclusion, the nominal working region is the one delimited by the two arrows.
The same study has been carried out for all the initially considered P values, and an increase of the working region width was found for increasing values of the balloon pressure.
An equivalent working point analysis has been performed with regard to the tuning process of the end cells. In Fig. 11, a complete overview of the working region detection results is given.

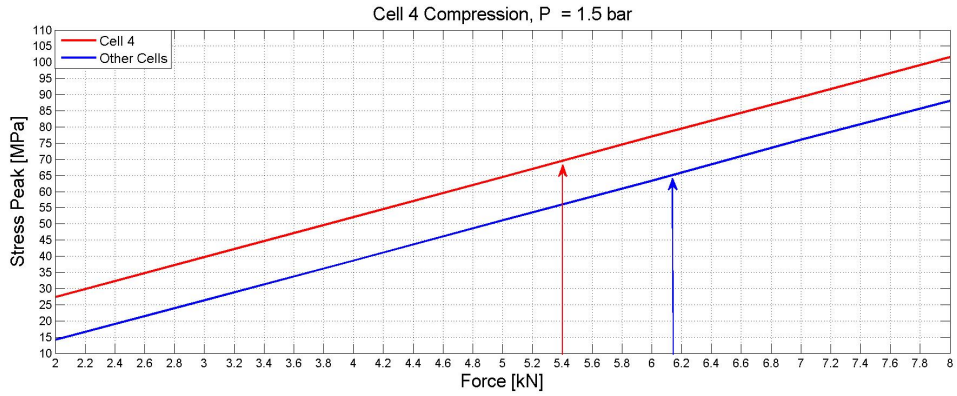

(a)

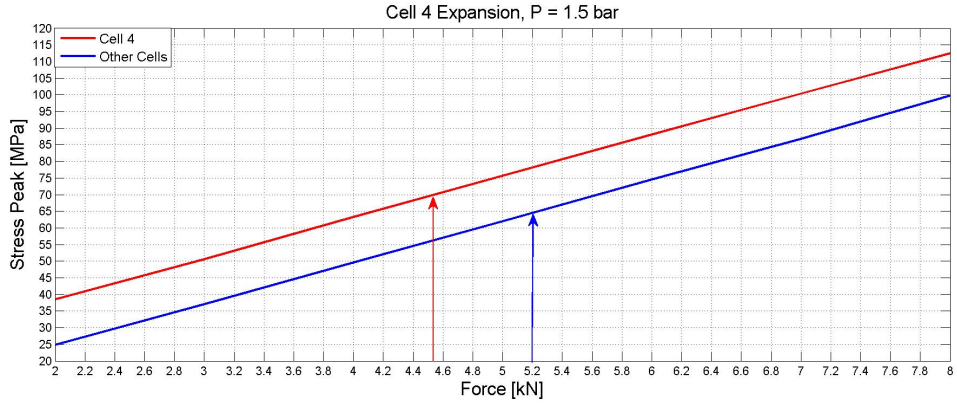

(b)

Figure 10: Working region detection for cell 4 compression (a) and expansion (b); P = 1.5 bar.

Pressure (bar)	Working Region (kN) Compression	
	Middle Cell	End Cell
1.5	5.40 – 6.15	5.55 – 6.10
2	5.35 – 6.40	5.48 – 6.40
2.5	5.30 – 6.70	5.40 – 6.70

(a)

Pressure (bar)	Working Region (kN) Expansion	
	Middle Cell	End Cell
1.5	4.52 – 5.20	4.65 – 5.20
2	4.20 – 5.20	4.30 – 5.20
2.5	3.80 – 5.20	3.90 – 5.20

(b)

Figure 11: Overview of the acceptable force ranges for cell compression (a) and expansion (b) depending on the balloon pressure.

2.2 Multiphysics analysis

A Multiphysics Analysis was required to provide a primitive description of how the resonant frequency changes during the loading process. Since the whole cavity consists of nine independent series-connected resonators, the electromagnetic field may resonate inside in nine different modes. For a proper particle acceleration, the Pi mode must be selected. Pi mode brings to a condition where fields in adjacent cells are Pi radians out of phase with each other and the particle itself crosses a cell in one-half of an RF period. In this way, every single cell gives a contribution to the acceleration process.
The nominal cavity model at rest shows a Pi mode eigenfrequency equal to 1.3006 GHz. Fig. 12 illustrates the internal field distribution for a loading process with a 2 bar balloon pressure and a 5 kN compression force. In Fig. 13, the difference between the loading

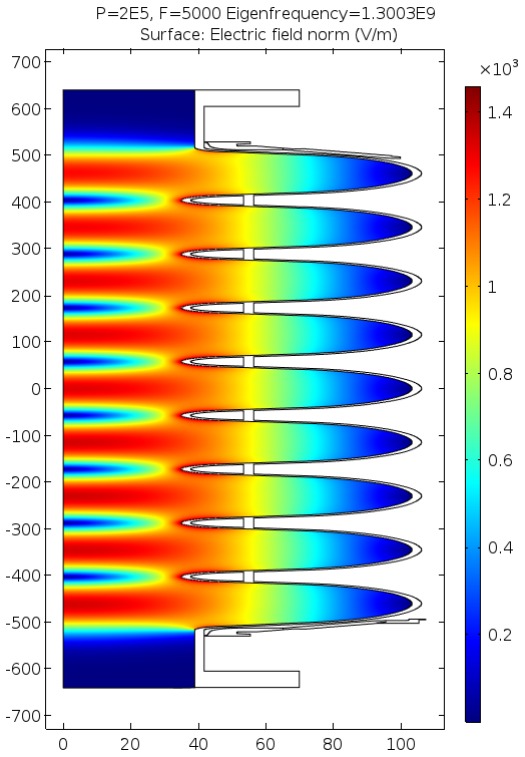

Figure 12: Pi mode internal field distribution during the loading process; P = 2 bar and F = 5 kN

process Pi mode eigenfrequency and the rest Pi mode eigenfrequency is shown as a function of the external force. A positive frequency shift is produced in the expansion test, while a negative one is produced in the compression test, as expected. A parametric sweep analysis has brought us to conclude that no significant differences can be noticed in the frequency shift over a balloon pressure variation. The estimated frequency shift is approximately of the order of 0.1 MHz per kN. Nevertheless, this is not a reliable result if the permanent frequency shift is the object of our investigation, since an elastic recovery should be taken into account when the applied force is removed. Some experimental tests have been performed in order to produce a precise estimation of the permanent frequency shift and study how the cell field amplitude changes at the same time (Sec. 3.5).

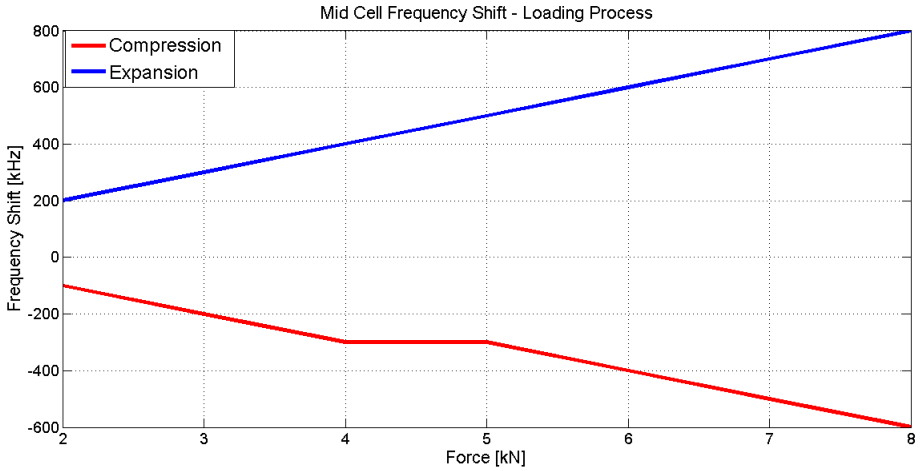

Figure 13: Frequency shift produced during the mid cell loading process.

3 Experimental tests

An experimental validation was required to verify the procedure feasibility as well as the expected results. As a first step, a preliminary study of the balloon material properties was performed. Then, a pressure test was carried out so as to qualify a 1-cell balloon for a 2 bar pressurization. As a conclusion, a tuning operation was attempted in order to understand if the Balloon Tuning Technique really produces the desired effects.

3.1 Balloon material qualification

A tensile test was made on three samples of the balloon material, i.e. rubberized nylon. The sample shape preparation has required a careful analysis, with the aim of avoiding stress concentration and eventually failure in non significant points. A specific design for the end part of the sample was needed to guarantee the reliability of the tensile tests, as shown in Fig. 14.

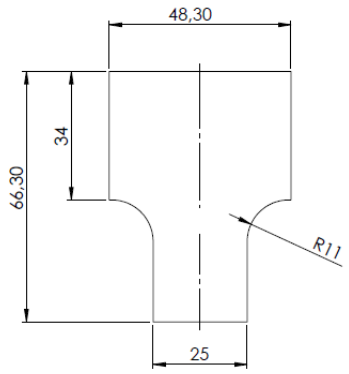

Figure 14: Design of the balloon material sample terminal part.

The initial geometrical properties of the material samples are reported in Fig. 15.
Each sample was directly cut from a 2-cell balloon, which had been assembled by an external vendor using four different pieces of rubberized nylon; those pieces were connected by glue links just at the cell equator and at the iris between the two adjacent cells. As a result, the tested samples consisted of four different segments connected with each other through three glue links, as shown in Fig. 16. Those linking edges were definitely the ones where the

Initial geometrical properties [mm]		
Length	Width	Thickness
151	25	0.27

Figure 15: Initial geometrical properties of balloon material samples.

failure was expected, and for this reason their inclusion in the tested samples was crucial in order to foresee the balloon behavior. The tensile test machine was controlled by means of

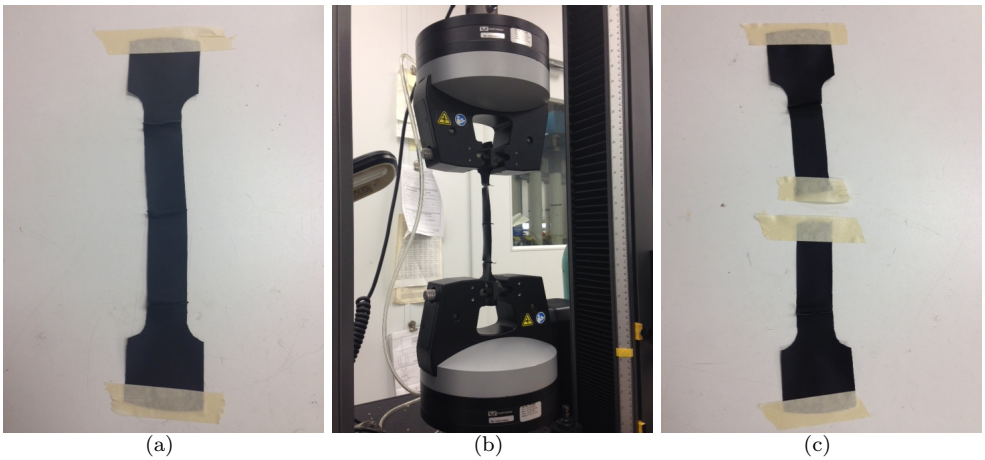

(a) (b) (c)

Figure 16: Rubberized nylon sample before (a) during (b) and after (c) the tensile test.

Bluehill Software; all the tests were carried out at room temperature, with a tensile extension velocity equal to 2 mm/min.
In Fig. 17, the load applied by the machine is plotted as a function of the tensile extension (a); the most interesting results of the tensile test are summarized as well (b). The glue links have shown a surprising resistance during the test, as the stress at break of the samples is approximately equal to 15 MPa.
Nevertheless, it is easy to understand that the properties of the material itself should also be investigated using samples without the glue links. Therefore, some more tensile tests were performed on pure material samples, not including the above mentioned glue links. The breaking stress found in the latter case is 65 MPa, and this value represents a more faithful characterization of the rubberized nylon resistance.
The stress produced on our 1-cell balloon surface by a 2 bar pressurization has been estimated equal to 25 MPa. A similar value may brought us to conclude that a balloon failure should occur while attempting to approach a close to 2 bar working point. However, this quick analysis has not considered that the balloon was purposely designed a bit bigger than the hosting cell, so as to ensure a load removal from the balloon to the cell surface. For this reason, one further experimental step was required to qualify the balloon even after these tensile tests (Sec. 3.2).
The tensile test has been reproduced on a set of different plastic materials, so as to discover possible alternatives to be used in the balloon fabrication. Following the same method, a characterization of four more materials has been produced:

- ATL 794A
- ATL 516-20
- ATL 516-10
- PVDF 889-10.

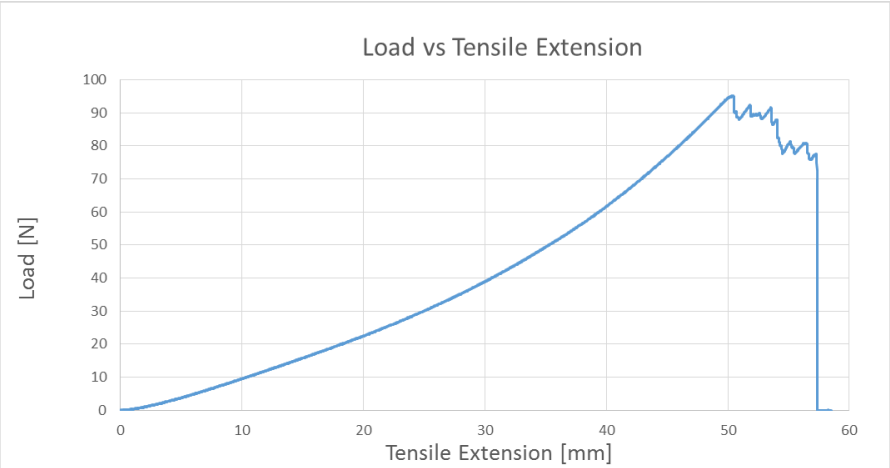

(a)

Test results		
Maximum Load [N]	Maximum Tensile Extension [mm]	Percent Elongation at Break
95.12	58.50	38.74%

(b)

Figure 17: Tensile test on balloon material sample. Load versus tensile extension plot (a), table of results (b).

As illustrated in Fig. 18, ATL 516-20 and PVDF 889-10 may represent an interesting alternative to rubberized nylon because of their exceptional grade of ductility.

3.2 Pressure test on a 1-cell balloon

A test was performed in order to qualify the 1-cell balloon for a 2 bar pressurization. The experimental procedure was studied so as to meet the Fermilab safety requirements, and a Hazard Analysis form was approved by some members of the safety office.
The experiment took place in a controlled access room, Lab 2. The lower flange of a 1-cell 1.3 GHz cavity (NR005) was fixed on a support. The deflated balloon was then folded and inserted into the cavity cell, as shown in Fig. 19. The balloon was connected to an elastic air flow pipe, experimentally qualified to bear a pressure of 2 bar. A pressure gauge was used to display the pressure value achieved during the inflating process, while a strain gauge was placed on the higher flange of the cavity with the aim of monitoring the structure axial displacement produced by the balloon pressurization.
During the inflating process, the pressure was controlled and limited by means of a pressure regulator and a relief valve, both linked to the nitrogen gas bottle. The pressure was gradually increased by a step of 0.1 bar. The pressurization was stopped for five minutes when the achieved pressure value was equal to 1, 1.5 and 2 bar, respectively. As a result, the rubberized nylon balloon was qualified for a 2 bar pressurization.
Moreover, a numerical simulation was performed so as to check the measured values of the cavity axial displacement. Since the cavity had previously undergone a chemical treatment, the real thickness was inferior than the one reported in the simulation nominal geometry. Therefore, the real thickness was directly measured on the cavity by means of an ultrasound probe, as shown in Fig. 20 (a), and a thickness correction was made on the nominal geometry CAD model. As a result, an acceptable matching between the measured values of the cavity axial displacement and the output produced by the simulation was achieved (Fig. 20).

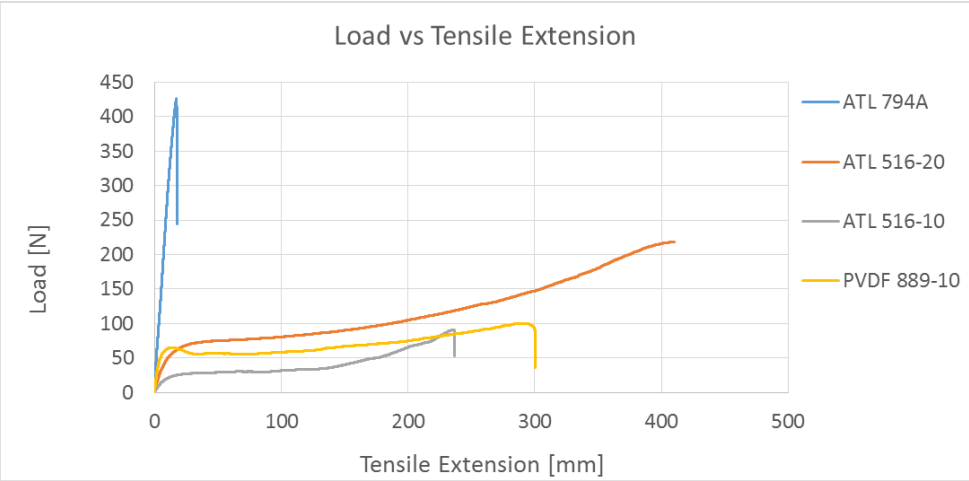

(a)

	Initial geometrical values [mm]			Test results		
	Length	Width	Thickness	Max. Load [N]	Max. Tensile Extension [mm]	% Break Elong.
ATL-794A	89	25	0.31	425.80	17.49	20.34%
ATL 516-20	85	25	0.56	217.84	410.18	482.57%
ATL 516-10	73	25	0.28	90.80	236.83	324.42%
PVDF 889-10	72	25	0.23	99.80	300.736	417.69%

(b)

Figure 18: Tensile test on alternative plastic materials. Load versus tensile extension plot (a), table of results (b).

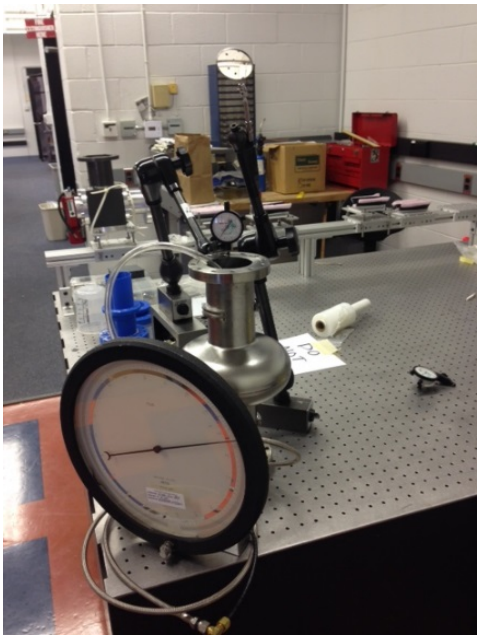

Figure 19: Experimental setup of the 1-cell balloon pressure test.

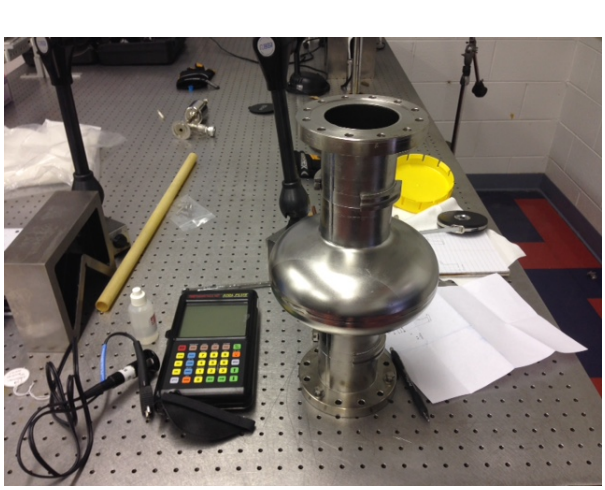

(a)

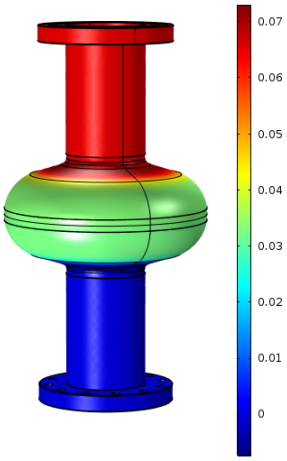

(b)

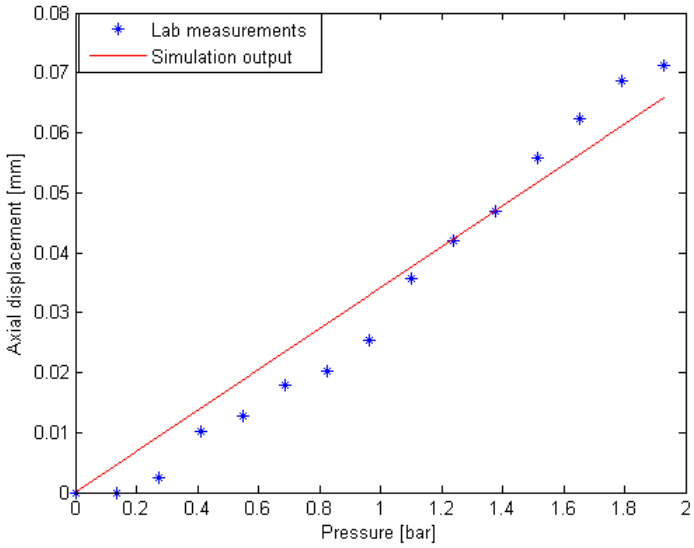

(c)

Figure 20: 1-cell balloon pressure test. Measurement of the cavity real thickness by means of an ultra-sound probe (a); 3D plot of the axial displacement estimated by the COMSOL simulation (b); comparison between simulation and experimental results (c).

3.3 Preliminary measurement of a 9-cell 1.3 GHz cavity parameters

Experimental tests have been done using a bare cavity to compare the effect of this novel tuning scheme with the existing one and calibrate the instrumentation. In future stages, the proposed tuning solution will be validated on a dressed cavity, which is the Balloon Tuning Technique real target.

A primitive tuning has been attempted on a bare 9-cell 1.3 GHz cavity (NR002) and thus a preliminary measurement of the cavity parameters was required. The NR002 cavity preliminary characterization was performed in a controlled access room, Lab 2; a network analyzer, RF antennas, the complete bead-pull measurement setup and the motor controllers were used so as to detect the cavity resonant frequency and the field profile along the cavity axis [3], [4].

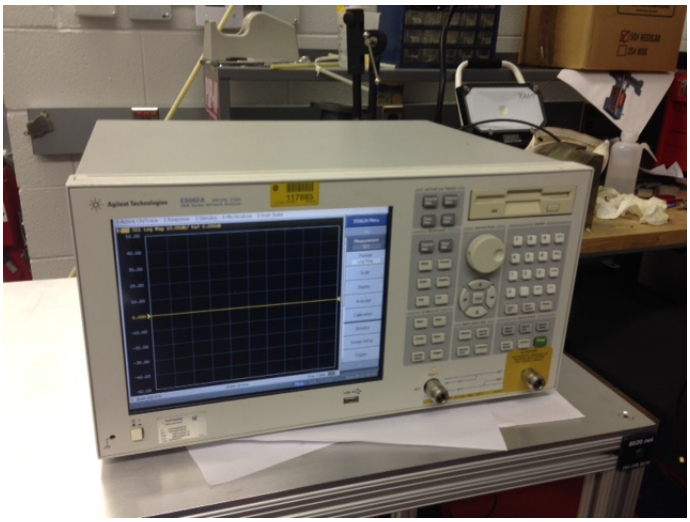

(a)

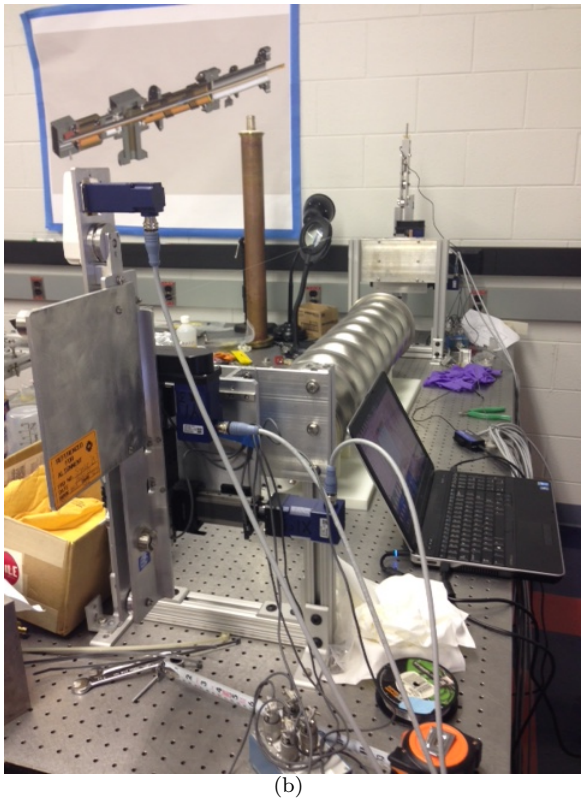

(b)

Figure 21: Network analyzer (a) and bead-pull real time data acquisition (b).

The resonant frequency before applying any tuning was found equal to 1297.338 MHz. In Fig. 22, the on-axis field profile normalized by its maximum value is represented as a function of the cavity axial coordinate. According to its definition, the field flatness is given by the lowest peak value that we can find among the nine half-waves represented in Fig. 22, i.e. 0.88. Since a proper cavity operation typically requires a field flatness value greater than 0.9, that cavity would not be usable without a preparatory tuning.

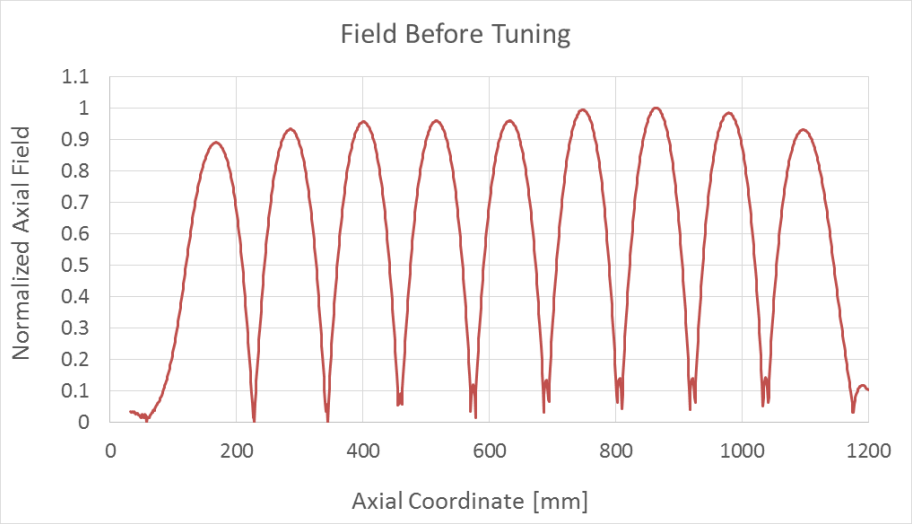

Figure 22: Normalized axial field of the bare 9-cell 1.3 GHz cavity before the tuning.

3.4 Tuning test: mid cell expansion

An expansion test was attempted on cell 2 of our 9-cell 1.3 GHz cavity, so as to increase the field amplitude inside that cell and the resonant frequency of the whole structure. To be precise, cell 1 experiences the lowest field peak among all the cells and for this reason it should have been selected as the targeted one. Nevertheless, at that stage of the validation process it was our interest to evaluate the method results without possible anomalies due to edge effect and asymmetry. This fact brought us to perform the expansion test on cell 2.
The cavity was placed on two V-supports and the deflated 1-cell balloon was inserted into cell 2. While one flange was fixed, the other one was connected to a hydraulic actuator which would have been used to apply the traction force during the test. Two load cells were used to have a better control of the applied load and to evaluate the effect produced by the friction between the supports and the table. Furthermore, four strain gauges were used to estimate the residual plastic deformation produced on the cavity after the tuning procedure. The test setup is represented in Fig 23.
The balloon was connected to the nitrogen bottle and externally pressurized up to 2 bar, and then a 4.2 kN traction force was gradually applied by the hydraulic actuator to the chosen flange. Since no significant difference was found between the load values reported by the two load cells, we may assume that the friction effect was negligible. At some intermediate points of the loading process, the strain gauge outputs were read and recorded, as shown in Fig. 24. After the traction force achieved the target value of 4.2 kN, the load was released. Considering the results reported in Fig. 24, a permanent increase in the cavity axial dimension has been estimated equal to 480 μm.
At this point, the measurement of the cavity parameters was repeated after the tuning, to verify the existence of the expected changes in both frequency and field flatness.

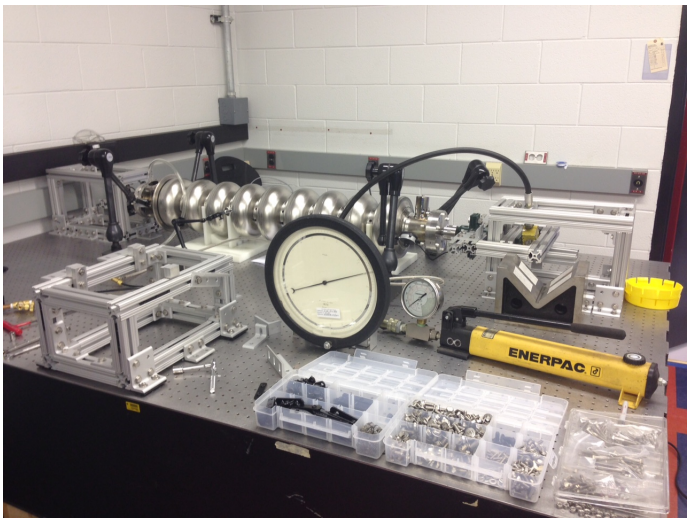

(a)

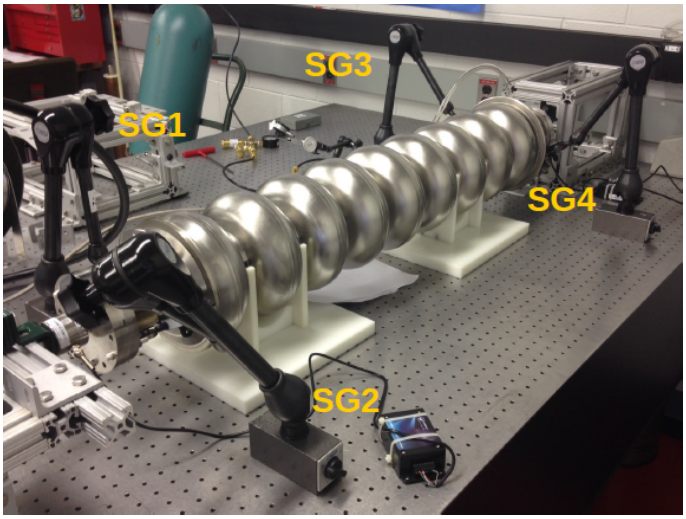

(b)

Figure 23: Cell 2 expansion test. Complete setup (a) and strain gauge positioning (b).

Traction Force [kN]	Measured displacement [mm]			
	SG1	SG2	SG3	SG4
0.222	0	0	0	0
0.663	5.283	4.953	2.794	3.658
1.334	11.176	14.224	6.096	7.874
2.064	18.085	15.621	9.119	9.017
4.180	Out of range	Out of range	18.669	17.907
0.222	5.436	3.397	4.572	3.302

Figure 24: Axial displacement values recorded by the strain gauge set during the loading process.

3.5 Results

After the tuning, the measured resonant frequency was equal to 1297.379 MHz. The tuning test produced a 40 kHz frequency shift, which is slightly lower than the value expected for this specific cavity. Nevertheless, the final frequency measurement was performed in a humid day and for this reason a few tens of kHz should be added to the measured frequency shift while estimating the real one. In the end, the test confirmed that our tuning procedure is able to produce a frequency shift which is comparable with the one produced by the classic tuning techniques. Such a remarkable result constitutes a first experimental evidence of our method validity from a frequency standpoint.
Moreover, the analysis of the changed normalized axial field profile has been performed again by means of the classic bead-pull measurement. The change in the field profile produced by cell 2 expansion test is shown in Fig. 25 (a).

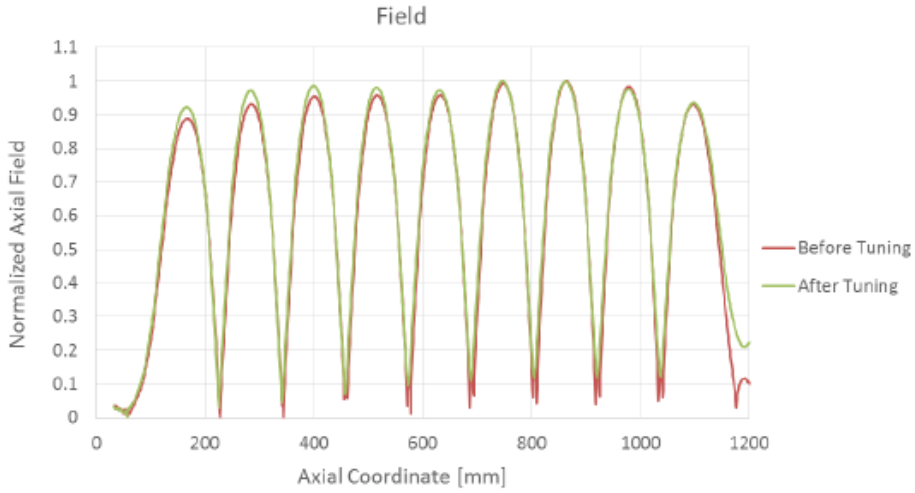

(a)

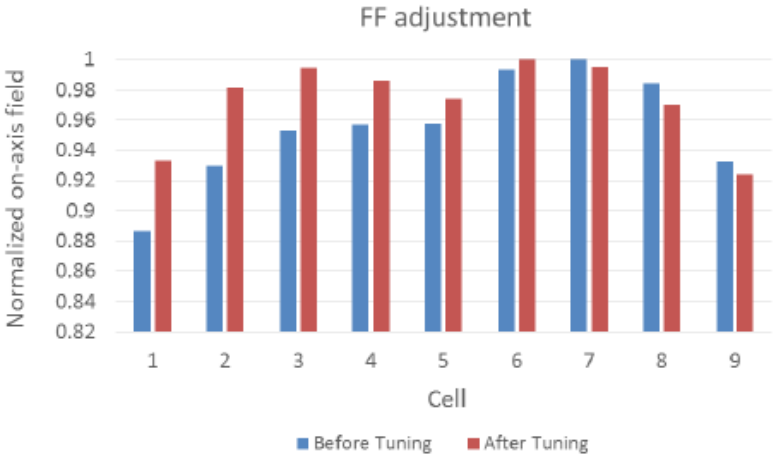

(b)

Figure 25: Normalized axial field before and after the tuning: profile (a) and cell peak amplitude (b).

The field flatness after the tuning is 0.93, so a 5% increase has been produced by the test and the cavity would be acceptable for operation as a result.
As previously stated, the original goal of the Balloon Tuning Technique is to control the deformation of each single cell, so as to change the field profile cell by cell using an iterative

procedure. The whole mechanism is based on a differential stress capable of producing a permanent change of the targeted cell iris-to-iris distance and aimed at guaranteeing a complete elastic recovery in all the other cells. For this reason, the optimal result would have been to observe a change in the field profile only in the targeted cell, i.e. cell 2. As shown in Fig. 25 (b), the field peak amplitude does not remain unchanged in all the other cells and a slight discrepancy between the ideal and real results is observed. In fact, a modification in the field peak amplitude has been found equal to

- +5% in cells 1-3
- +1.5% in cells 4-5
- -0.06% in cells 6-9.

The targeted cell experiences the highest change in the field amplitude, but also the adjacent ones (1 and 3) show a similar behavior. This is a side effect also produced in other classic tuning techniques. Since the iris is a point shared between adjacent cells, we may expect that acting on the targeted cell iris will modify in some way also the properties of the adjacent ones. As a conclusion, the uniform behavior shown by cells 1-3 should not be that surprising. Furthermore, a positive result comes when looking at the change in cells 6-9. In this case, a negligible modification has been produced by the tuning and this result is very close to the ideal desired effect. A 1.5% increase in the cell 4 and 5 field amplitude is lower than the percent change observed in cells 1-3, but still relevant. It might suggest that some slight plastic deformation have occurred also in these non-targeted cells while the test was in execution. And this is probably due to the fact that a 4.2 kN traction force was too high. The working point analysis, indeed, had been made using the nominal geometry of the cavity. The change in the material properties and the cavity thickness determined by the chemical treatments had not been taken into account.

4 Conclusion

A first validation of the Balloon Tuning Technique concept has been achieved, by means of both a Finite Element Analysis and experimental tests. The proposed approach is effective when a frequency retuning and a field flatness enhancement are needed; the control on each single cell deformation has not been completely proven to be a feature of this technique, but the results achieved in the final tuning test have given an encouraging sign in this direction.

4.1 Future studies

Some more steps are needed to proceed in validating the Balloon Tuning Technique concept. First, the loading process should be studied by means of a non linear and time dependent multiphysics simulation. Including the non linear behavior shown by the cavity material over its yield stress would give a significant contribution to have a better understanding of the plastic deformation effect. On the other hand, a time dependent simulation would better represent the loading process itself, with the external force and the balloon pressure being removed after the test. As a result, a more precise evaluation of the permanent effect produced on the cavity by the tuning procedure could be achieved, from a mechanical, frequency and field amplitude standpoint.
In addition to that, the nominal geometry of the 9-cell cavity should be replaced with the real one in the next simulations. Such a correction would help to minimize the difference between the experimental results and the simulation outputs. A correction in the cavity thickness, as well as in the niobium Young Modulus, would bring to a new and more accurate selection of the procedure working point region. On this regard, the Young Modulus used for niobium in the simulations was 105 GPa, but a more realistic value to use would be around 80 MPa. In the end, a similar experimental approach should be adopted in order to validate the concept also in the compression case, for both a mid cell and an end cell.
An efficient solution for the balloon insertion and removal should be found at this stage, to make the experimental phase easier.

5 References

[1] J.-H. Thie et al., *Mechanical Design of Automatic Cavity Tuning Machines*,
SRF Workshop - September 2009, Berlin, Germany
http://bib-pubdb1.desy.de/record/92712/files/THPPO074.pdf/

[2] H. Jiang et al., *Mechanical Properties of High RRR Niobium with Different Texture*,
IEEE Transactions on Applied Superconductivity, 2007, Volume: 17, Issue: 2
www.nscl.msu.edu/~hartung/phptry/papers/ASC06_4LJ06.pdf

[3] P. Schmuser, *Tuning of Multi-Cell Cavities using Bead Pull Measurements*
http://www.lns.cornell.edu/public/SRF/1992/SRF920925-10/SRF920925-10.pdf

[4] S.-W. Lee, *Bead-Pulling Measurement (Multi-Cell Cavity Field Flatness)*
http://uspas.fnal.gov/materials/08UMD/SRF/Bead-Pulling.pdf